Influence of Regioirregular Structural Units on the Crystallization of Isotactic Polypropylene

ANTONIO MARIGO,[1] CARLA MAREGA,[1] ROBERTA SAINI,[1] ISABELLA CAMURATI[2]

[1] Department of Inorganic, Metallorganic and Analytical Chemistry of the University, Via Loredan 4, 35131 Padova, Italy

[2] MONTELL Italia, Centro Ricerche "G. Natta," P. le Donegani 12, 44100 Ferrara, Italy

Received 28 December 1999; accepted 7 April 2000

ABSTRACT: Seven samples of isotactic polypropylene were examined to study the influence on the formation of the γ crystalline phase of possible regiodefects along the chain. Wide-angle X-ray diffraction allowed the determination of the percentage of the γ phase in the samples and ^{13}C-NMR spectroscopy was used to correlate the development of the γ phase with the existence of regioirregular structural units along the chain. Furthermore, it was possible to appraise the contributions given by the different families of lamellae to the small-angle X-ray diffraction patterns. © 2000 John Wiley & Sons, Inc. J Appl Polym Sci 79: 375–384, 2001

Key words: isotactic polypropylene; X-ray diffraction; NMR; crystallization; defects

INTRODUCTION

Isotactic polypropylene (i-PP) is one of the synthetic polymers with high commercial interest. Its history is relatively recent, since the catalyst process necessary for the reaction of polymerization was discovered in 1954 by Natta and coworkers.[1]

Since the beginning of its industrial production in 1957, i-PP has been competitive on the market; its easy processability as well as its notable purity and the availability of the monomer currently make it one of the most requested plastic materials all over the world. I-PP is a thermoplastic polymer, having a low specific weight and a high tensile strength, stiffness, and hardness. Besides, it has excellent dielectric properties, chemical inertia, and damp resistance, typical of the olefin polymers.

A particular characteristic of i-PP is its polymorphous behavior, as it is known that this polymer has three different crystalline phases, α, β, and γ[2]. The monoclinic α phase is the best known and the most common crystalline state of the polymer. On the other hand, various authors showed that the hexagonal β phase and the triclinic γ phase can be obtained only in particular conditions. For example, the γ form can be obtained as a result of crystallization under elevated pressures[3,4] or from i-PP samples with a low molecular weight.[5–7] Random copolymers of propylene with other olefins (ethylene and 1-butene) can crystallize in the γ phase.[8–12] In particular, Zannetti and coworkers[9] found that the content of the γ form increases as the amount of the comonomer in the chain increases. These results are in good agreement with the observations of Turner Jones,[8] who reported that the development of the γ phase in copolymers can be related to the interruptions in the isotactic chain, due to the insertion of the comonomer.

Recently, high percentages of the γ form have been found in i-PP samples synthesized with zirconocene-based homogeneous catalysts.[13–15] These catalytic systems introduce some regioir-

Correspondence to: A. Marigo.

Journal of Applied Polymer Science, Vol. 79, 375–384 (2001)

Table I Analyzed i-PP Samples and the Catalytic Systems Used for Their Preparation

Sample	Catalytic System[a]
M1	rac-(EBI)$ZrCl_2$/MAO
M2	rac-(EBI)$ZrCl_2$/MAO
M3	rac-(EBDMI)$ZrCl_2$/MAO
M4	rac-(EBDMI)$ZrCl_2$/MAO
M5	rac-(EBTHI)$ZrCl_2$/MAO
G1	$MgCl_2$/$TiCl_4$/diether–$AlEt_3$
G2	$MgCl_2$/$TiCl_4$/diether–$AlEt_3$

[a] EBI, ethylene bis(1-indenyl); EBDMI, ethylene bis(4,7-dimethyl-1-indenyl); EBTHI, ethylene bis(4,5,6,7-tetrahydro-1-indenyl).

regular units along the chain, deriving from 2,1 and 3,1 insertions.[16–20] Therefore, it appears that the polypropylene microstructure plays an important role in the crystallization of the polymer.

The aim of this work was to investigate the effect of regiodefects on the formation of the γ crystalline phase and to evaluate the influence of the γ-form amount on some parameters related to the lamellar structure. This was performed by analyzing the i-PP samples using wide- and small-angle X-ray diffraction (WAXS and SAXS, respectively) and ^{13}C-NMR spectroscopy.

EXPERIMENTAL

Samples

The analyzed samples of i-PP are shown in Table I together with the catalysts used for their preparation. Samples M1–M5 were synthesised using homogeneous zirconocene-based catalysts, while samples G1 and G2 are fractions of a polymer produced with a heterogeneous Ziegler–Natta catalyst. The G1 and G2 samples were obtained using the TREF (temperature rising elution fractionation) technique, which allows separation of the macromolecules according to their crystallizability. They differ in molecular weight and stereoregularity.

The polymer sample, obtained as a powder, was heated over the melting temperature, and after a slow cooling to 20°C, a thin rectangular small plate (thickness 0.06 cm) was obtained. The intrinsic viscosity ([η]), the viscosimetric-average molecular weight ($\bar{M}_v$), and the melting temperature (T_m) were determined for the examined samples. The values are collected in Table II.

Wide-angle X-ray Scattering

The WAXS patterns were recorded in the diffraction angular range of 10–50° 2θ, using a GD 2000 transmission diffractometer produced by Ital Structures, working in the Seemann–Bohlin geometry, and with a quartz crystal monochromator of the Johansson type on the primary X-ray beam: CuKα_1 radiation was used.

The application of the least-squares fit procedure elaborated by Hindeleh and Johnson[21] gave the crystallinities by weight, and then they were transformed into volume crystallinities, Φ_{WAXS}.[22] The α and γ polymorphous structures of i-PP were characterized by different crystalline structures; consequently, the wide-angle diffraction spectra of the two pure phases are also different.

The substantial difference between the WAXS spectrum of the i-PP crystallized in the α form and that of the γ form is the existence of a peak at 18.6° 2θ in the first one, substituted in the second by a reflex of 20.1° 2θ, absent in the first one [see Fig. 1(a,b)]. The diffraction spectrum of a sample containing both the crystalline phases has all peaks typical of the two forms. Using the WAXS spectra, it is therefore possible to determine the relative amount of the crystalline phase in the γ form.[12]

Small-angle X-ray Scattering

The SAXS patterns were recorded by an MBraun system, using CuKα radiation from a Philips PW 1830 X-ray generator. The data were collected using a position-sensitive detector, in the scattering angular range of 0.1–5.0° (2θ), and were afterward corrected for blank scattering.

A constant continuous background scattering was then subtracted[23] and the obtained intensity

Table II Intrinsic Viscosity ([η]), Average Viscosimetric Molecular Weight ($\bar{M}_v$), and Melting Temperature (T_m) of the Analyzed i-PP Samples

Sample	[η] (dL/g)	$\bar{M}_v$	T_m (°C)
M1	0.61	53,600	145
M2	0.47	37,700	139
M3	0.15	8,100	132
M4	0.14	7,300	123
M5	0.39	29,300	137
G1	0.68	62,100	162
G2	0.45	35,600	160

values $\tilde{I}(s)$ were smoothed in the tail region, with the aid of the $s \times \tilde{I}(s)$ versus $1/s^2$ plot.[24] Finally, the Vonk's desmearing procedure[25] was applied and the one-dimensional scattering function was obtained by the Lorentz correction $I_1(s) = 4\pi s^2 I(s)$, where $I_1(s)$ is the one-dimensional scattering function, and $I(s)$, the desmeared intensity function, being $s = (2/\lambda) \sin \theta$.

Theoretical Evaluation of the SAXS Patterns

The evaluation of the SAXS patterns, according to some theoretical distribution models,[26,27] was carried out referring to the Hosemann model,[28] which assumes the presence of lamellar stacks having an infinite side dimension. This assumption, in practice, takes into account a monodimensional electron density change along the direction normal to the lamellae. According to this model, the intensity profile is expressed as follows:

$$I(s) = I'(s) + I''(s) \tag{1}$$

where

$$I'(s) = \frac{(\rho_c - \rho_a)^2}{4\pi^2 s^2 D} \quad \frac{\begin{array}{c}|1 - F_C|^2(1 - |F_A|^2) \\ + |1 - F_A|^2(1 - |F_C|^2)\end{array}}{|1 - F_C F_A|^2} \tag{2}$$

$$I''(s) = \frac{(\rho_c - \rho_a)^2}{2\pi^2 s^2 DN} Re\left\{\frac{F_A(1 - F_C)^2(1 - (F_A F_C)^N)}{(1 - F_A F_C)^2}\right\} \tag{3}$$

In these equations, F_C and F_A represent the Fourier transforms of the distribution functions of the lamellar thickness C and of the amorphous regions A; ρ_c and ρ_a are, respectively, the electron densities of the crystalline and amorphous regions; and N is the number of the lamellae in the stack, and D, the average long period.

The optimized parameters were the average lamellar thickness C, the distribution standard deviation of the lamellar thickness σ_C, $\Phi_{SAXS} = C/D$, and N. The average thickness of the amorphous regions $A = [(1 - \Phi_{SAXS})/\Phi_{SAXS}]C$ and its distribution standard deviation $\sigma_A = (\sigma_C/C)A$ were calculated using the optimized parameters.

Nuclear Magnetic Resonance

The solution ^{13}C-NMR spectra of the polymer samples were recorded with a Bruker DPX 400 spectrometer operating in Fourier transform mode at a frequency of 100.61 MHz. Spectra were acquired at 120°C in dideuterated 1,1,2,2-tetrachloroethane, applying a 90° pulse, with 12 s of delay between pulses, and CPD (waltz 16) to remove ^{1}H–^{13}C coupling. The signal of the *mmmm* pentad at 21.8 ppm was used as an internal reference.

The ^{13}C-NMR spectra of the M1 and M3 samples are shown in Figure 2(a,b). In the methyl region of the ^{13}C-NMR spectrum of i-PP, the resonance peaks due to different steric sequences, made up of five monomeric units called pentads,[29–31] are present. The percentage of the *mmmm* pentad is taken as a measure of the isotacticity of the investigated polymers.

Owing to the presence of regioirregularities, the content of the *mmmm* pentad of the samples synthesized with zirconoceres was determined assuming that the polymerization follows the "enantiomorphic site" statistical model using the method described in ref. 32. On the other hand, the percentage of *mmmm* pentad of the samples from heterogeneous catalysis was calculated considering that the only sequences existing in meaningful quantity, besides the *mmmm*, are the *mmmr*, *mmrr*, and *mrrm* pentads having an *mmmr*:*mmrr*:*mrrm* = 2:2:1 intensity ratio. The following expression was then used:

$$mmmm = 100 - 5mrrm \tag{4}$$

From the ^{13}C-NMR spectra of the samples of i-PP, the percentages of regio-irregular structural units along the chain, due to insertions of the types 2,1 and 3,1,[16–20] were calculated as reported in ref. 32.

RESULTS AND DISCUSSION

The acquisition and the elaboration of the WAXS spectra allowed the determination of the weight crystallinity degree, from which the volumetric crystallinity can be obtained, using the density values for crystalline and amorphous phases reported in the literature[2] ($\rho_c = 0.94$ g/cm^3; $\rho_a = 0.865$ g/cm^3). The percentage of the crystalline phase in the γ form was also calculated. These data for the powders and thin plates are reported in Tables III and IV, respectively.

It can be noticed that for every sample the thin plate has a higher degree of crystallinity with

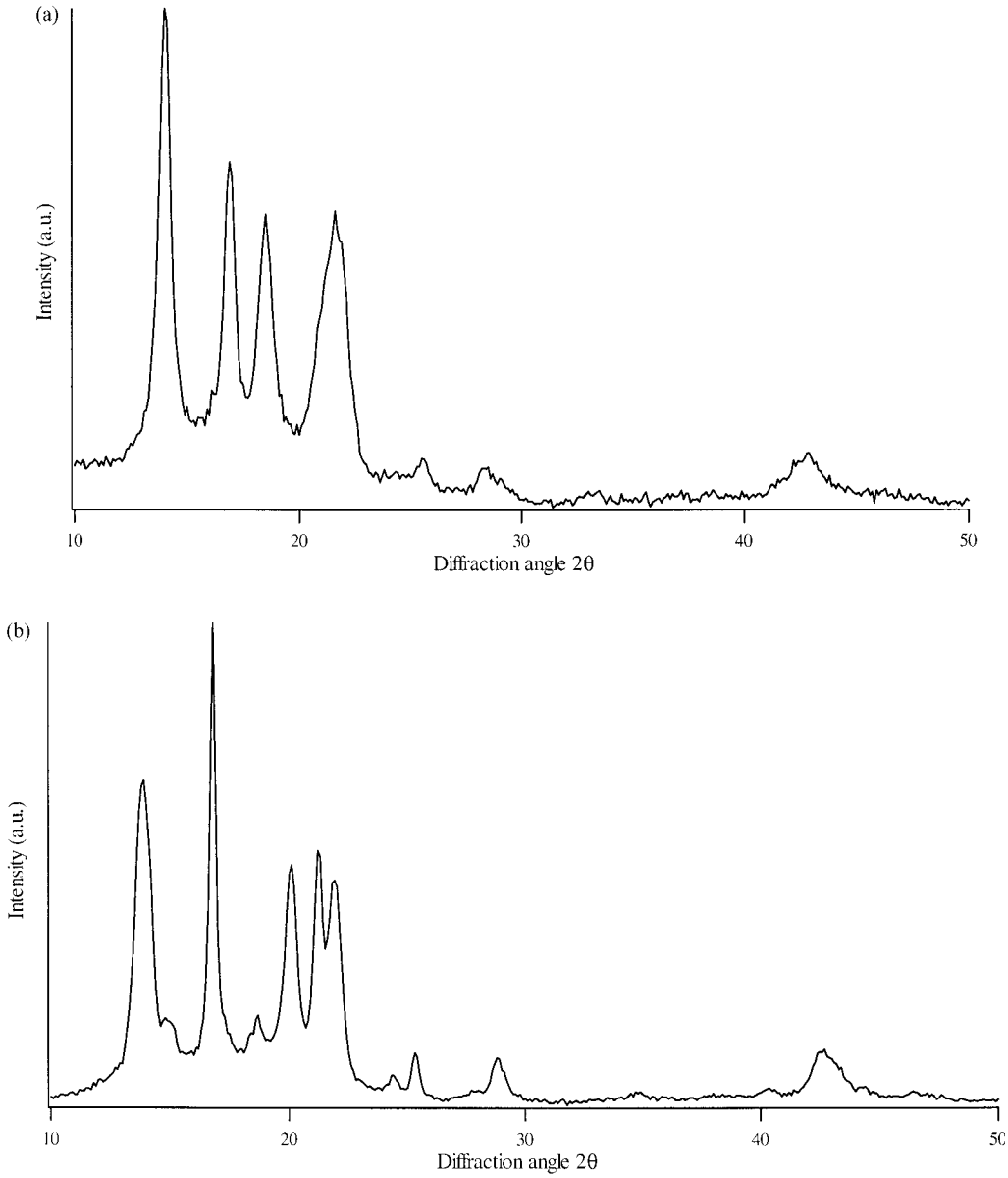

Figure 1 (a) WAXS spectrum of sample M2 (powder); (b) WAXS spectrum of sample M2 (plate).

respect to the powder. This can be explained considering that the thin plates were prepared by melting and subsequent slow cooling, allowing the macromolecules to settle themselves in a situation of greater order in comparison to the starting conditions. This leads to a crystallinity increase.

Table III shows that powders contain only the α form, except for the samples M3, M4, and M5, in which a certain percentage of the γ phase is present (less than 20%). Furthermore, the thin plates have a higher content of the γ form, with respect to the corresponding powders. This result is in agreement with the observations of Turner Jones,[8] who reported that the formation of the γ phase depends on the conditions of crystallization and is particularly favored by slow cooling.

The WAXS study also revealed that there is a notable difference, as far as the tendency to crystallize in γ form is concerned, between the polymers obtained with homogeneous catalysts and those resulting from heterogeneous catalysts. In

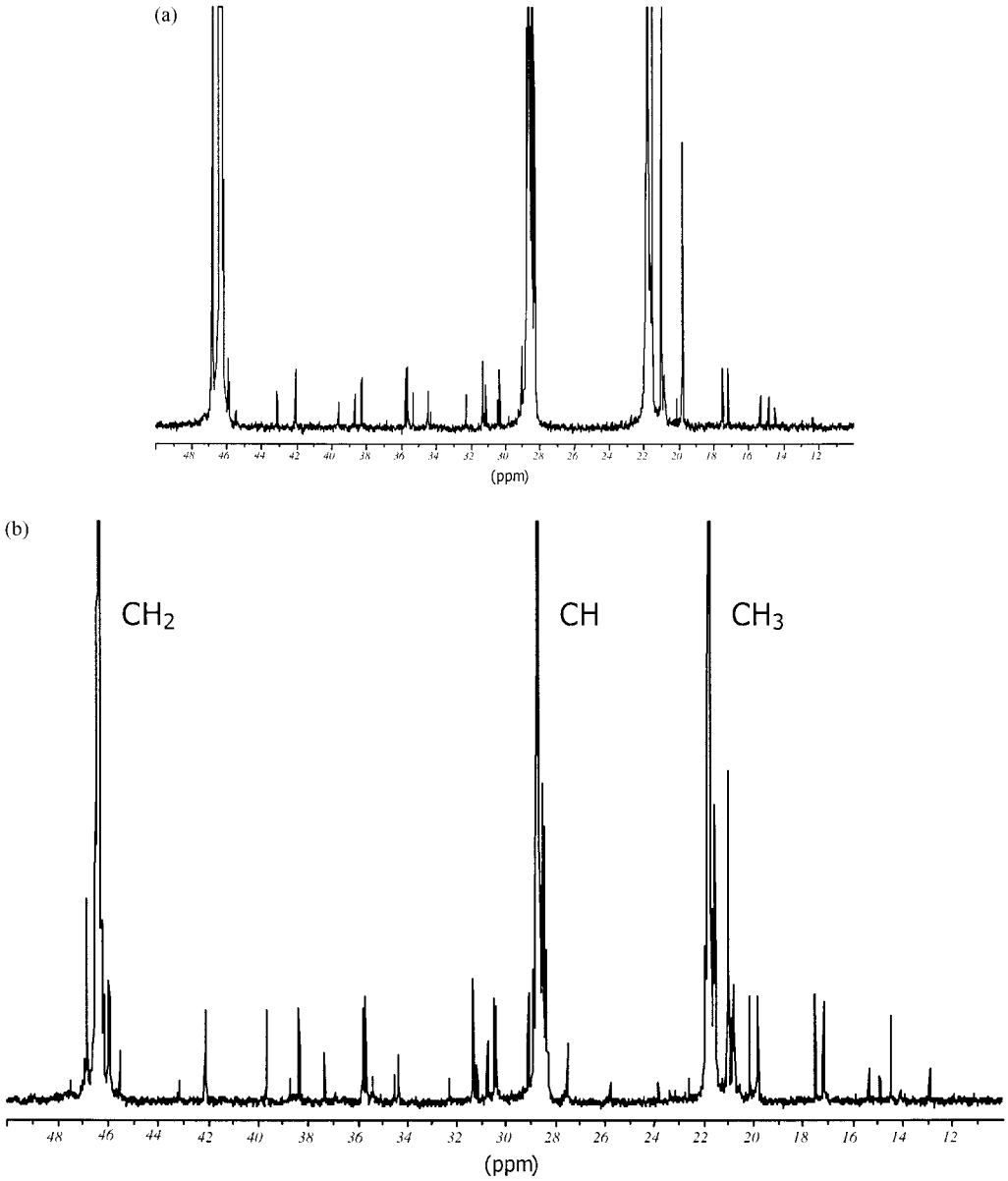

Figure 2 (a) ^{13}C-NMR spectrum of sample M1; (b) ^{13}C-NMR spectrum of sample M3.

fact, the thin plates of the i-PP samples synthesized with zirconocenes contain a much higher percentage of the γ phase in comparison to the thin plates of the polymers obtained by heterogeneous catalysis (G1 and G2).

In Figure 3, the percentage of the γ phase of the plates, with respect to the melting temperature, is shown. It clearly appears that, as the melting temperature decreases, the content of the γ form increases, as demonstrated by some previous studies.[14,15] Such behavior can be explained on the basis of the different melting temperatures characterizing the two polymorphous structures. In fact, the γ phase has a lower melting temperature in comparison to the α form.

In Table V, the percentages of regioirregular units (2,1 and 3,1) in the chain determined by the ^{13}C-NMR analysis are reported. It can be seen that, while the polymers synthesised with zirconocenes have regiodefects of types 2,1 and 3,1, in the two TREF fractions (G1 and G2) such defects are not found. All the polymers have a high isotacticity, samples G1 and G2 having the highest percentage of the *mmmm* pentad.

Now let us compare the results of the NMR analysis with those obtained using the WAXS

Table III Weight Crystallinity (X_c), Volumetric Crystallinity (Φ_{WAXS}), and Percentage of γ Form (C_γ) for the Powder i-PP Samples

Sample	X_c	Φ_{WAXS}	C_γ (%)
M1	0.58	0.56	0
M2	0.52	0.50	0
M3	0.57	0.55	6
M4	0.53	0.51	13
M5	0.53	0.51	19
G1	0.66	0.64	0
G2	0.66	0.64	0

Table IV Weight Crystallinity (X_c), Volumetric Crystallinity (Φ_{WAXS}), and Percentage of γ Form (C_γ) for the i-PP Samples in Plate

Sample	X_c	Φ_{WAXS}	C_γ (%)
M1	0.74	0.72	68
M2	0.69	0.67	84
M3	0.73	0.71	95
M4	0.67	0.65	96
M5	0.70	0.68	89
G1	0.74	0.72	28
G2	0.73	0.71	37

technique. The thin plates of the G1 and G2 samples, which do not have any regioirregularity, show a considerably smaller percentage of the γ phase in comparison to the other thin plates. This is true also for samples of a similar molecular weight as is evident comparing G1 with M1 or G2 with M2 and M5. Therefore, the existence of regiodefects in the chain favors the crystallization of i-PP in the γ phase. The regioirregular insertions cause interruptions in the polypropylene chain, which according to the literature,[8,9] are responsible for the development of the γ form. These results are also in accordance with the observations of Marigo et al.,[12] who, studying random copolymers of propylene with ethylene, already demonstrated the existence of defects having the same structure as that of the 3,1 ones, but derived from the insertion of the comonomer after a regioirregular propene unit, in samples able to crystallize in the γ form.

In the thin plates of the samples obtained from homogeneous catalysis, the content of the γ phase seems to increase as the percentage of regiodefects increases. Therefore, the existence of a direct proportionality between the percentage of the γ form and the number of "chain defects" can be hypothesized.

In fact, the samples having the higher content of the γ phase (nearly 100% in the thin plates) are the M3 and M4 samples presenting all the three types of defect. The high content of the γ form could also be due to their low molecular weight, as it was reported in the literature that polymers with a low molecular weight are able to give a high amount of the γ form.[5–7] The long-period values D_{Bragg} were directly determined from the scattering curve, by elaborating the SAXS profiles.

Both the thin plates and the powders were analyzed. For the powders, the formation of diffraction peaks was not observed. This can be ascribed to the existence in the powders of small lamellae, which are not organized in lamellar stacks. The D_{Bragg} values for the thin plates of the i-PP samples are shown in Table VI.

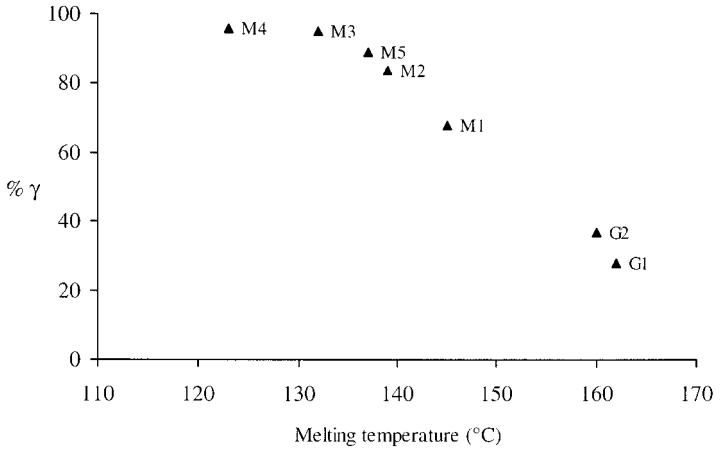

Figure 3 Percentage of γ phase as a function of the melting temperature.

Table V ^{13}C-NMR Analysis of the i-PP Samples

Sample	*mmmm* (%)	2,1E (%)	2,1T (%)	3,1 (%)
M1	91	0.25	0.14	0
M2	88	0.30	0.19	0
M3	92	0.94	0.24	0.24
M4	88	0.61	0.24	0.71
M5	91	0.14	0	0.80
G1	99	0	0	0
G2	99	0	0	0

Table VI Long-period Values (D_{Bragg}) Obtained for the i-PP Samples in Plate

Sample	D_{Bragg} (Å)
M1	139
M2	119
M3	119
M4	113
M5	119
G1	155
G2	139

The SAXS spectrum of the thin plate of the G1 sample (Fig. 4) is constituted by two partially superimposed peaks. Such a phenomenon is due to the existence of two populations of lamellar stacks, characterized by a different long period. The existence of superimposed signals requires the use of a technique able to consider the peaks with a certain degree of independence and having the purpose to evaluate their contribution to the total curve. A suitable procedure for an independent evaluation of the scattering signals is the calculation of the distribution that could lead us to reconsider some parameters such as, for instance, the position of the intensity maximums.

For the samples M2, M3, M4, and M5, the best fit was obtained using a "single-population model"; for the others, a "double-population model" gave a more satisfactory fit. The resulting fits for the thin plates of the G1 and M3 samples are shown in Figure 5(a,b), while the results obtained are collected in Table VII.

Examining the data of Tables IV and VII, it is possible to make some important observations. The samples showing a double population are those having the smallest content of the γ phase. The SAXS diffraction profiles of the other thin plates, showing a higher percentage of the γ form, and which were reconstructed using a single peak (single population), have periodicities comparable to that of population 2 in samples M1, G1, and G2. The fact that the analysis of the SAXS profile of the M2, M3, M4, and M5 thin plates needs a single distribution model is probably due to their high percentage of the γ phase, which prevents distinguishing the two populations (i.e., only the lamellae of the γ phase are visible).

We can therefore affirm that population 1 corresponds to the α phase, and population 2, to the γ phase. The two crystalline structures give rise to lamellar stacks characterized by a different periodicity. In particular, the α phase has a higher value of the long period in comparison to

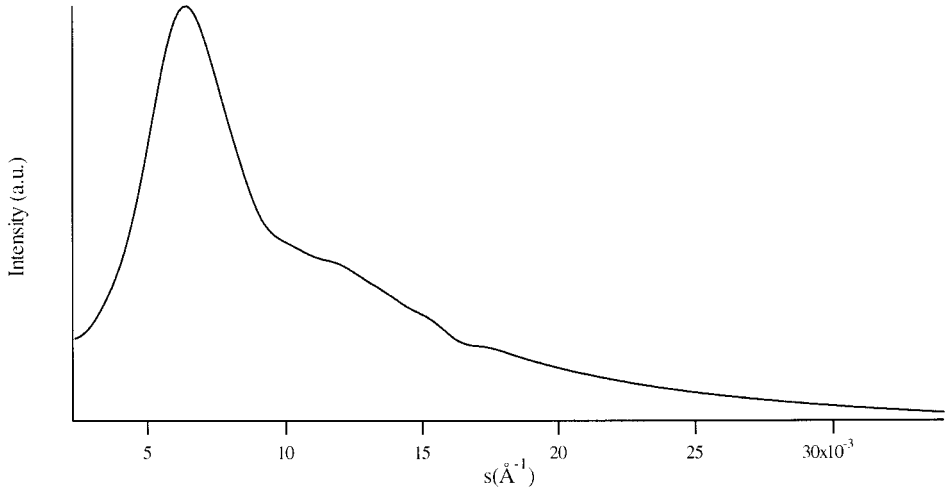

Figure 4 SAXS spectrum of the sample G1 (plate).

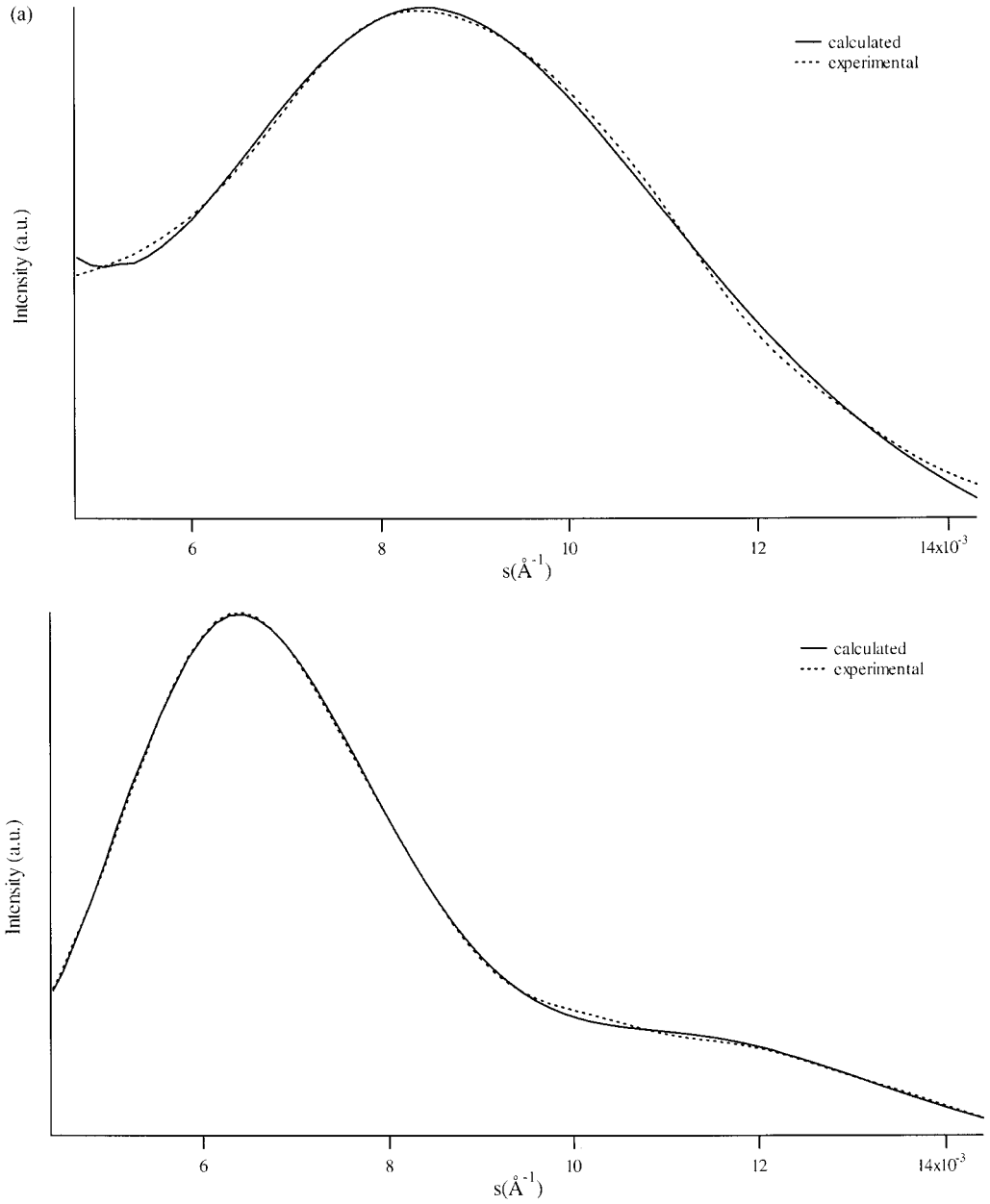

Figure 5 (a) Fit of the SAXS spectrum of sample M3 (plate); (b) fit of the SAXS spectrum of sample G1 (plate).

the γ form. Moreover, both the periodicity and the thickness of the crystalline layer (C) decrease, passing from the α phase to the γ phase.

In analyzing the results of the M1, G1 and G2 samples, as far as the distribution values are concerned, it can be noticed that population 1 (α form) has a narrower distribution of σ_C/C lamellar thickness in comparison to that of population 2 (γ form). The same is true for the σ_D/D distribution.

The calculation of the distribution of the lamellar thickness also allows us to evaluate the volumetric crystallinity of the thin plates. A comparison of the Φ_{WAXS} (Table IV) and Φ_{SAXS} values (Table VII) shows that the crystallinity obtained with the high angle is nearly equal to the one obtained with the small angle (Fig. 6).

It is now necessary to consider that the WAXS technique allows the detection of all the crystalline forms in the sample, while the SAXS analysis

Table VII Thickness of Crystalline (*C*) and Amorphous (*A*) Phases; Long Period (*D*), Thickness Distribution Values (σ_c/C and σ_D/D), and Volumetric Crystallinity (Φ_{SAXS})

Sample	C_1 (Å)	A_1 (Å)	D_1 (Å)	$\left(\frac{\sigma_C}{C}\right)_1$	$\left(\frac{\sigma_A}{A}\right)_1$	$\left(\frac{\sigma_D}{D}\right)_1$	C_2 (Å)	A_2 (Å)	D_2 (Å)	$\left(\frac{\sigma_C}{C}\right)_2$	$\left(\frac{\sigma_A}{A}\right)_2$	$\left(\frac{\sigma_D}{D}\right)_2$	Φ_{SAXS}
M1	85	33	118	0.34	0.34	0.26	76	30	106	0.49	0.49	0.38	0.72
M2							70	30	100	0.32	0.32	0.24	0.70
M3							67	32	99	0.48	0.48	0.36	0.68
M4							60	36	96	0.35	0.35	0.25	0.62
M5							69	33	102	0.34	0.34	0.25	0.67
G1	98	38	136	0.27	0.27	0.21	69	26	95	0.45	0.45	0.35	0.72
G2	85	33	118	0.26	0.26	0.20	76	29	105	0.49	0.49	0.38	0.72

The Pedice Values refer to the different lamellae families.

is only sensitive to the crystalline regions organized in lamellar stacks. Therefore, with $\Phi_{WAXS} \approx \Phi_{SAXS}$, it can be supposed that, in the case of the examined i-PP thin plates, all crystalline regions are organized in stacks.

CONCLUSIONS

X-ray diffraction techniques and ^{13}C-NMR spectroscopy appear to be definitely useful for the structural investigation of i-PP. The WAXS analysis confirmed that the i-PP samples synthesized with zirconocene-based homogeneous catalysts are able to give high percentages of the γ form. Besides, it was also observed that as the melting temperature decreases the content of the γ phase increases. The ^{13}C-NMR technique allowed the correlation of the development of the γ phase with the existence of regioirregular (2,1E, 2,1T and 3,1) units along the chain. These defects can cause interruptions in the isotactic sequences, which are probably responsible for the crystallization of i-PP in the γ form.

In the case of the SAXS technique, the study of the distribution of lamellar thickness was very helpful, allowing the independent evaluation of the contributions of different families of lamellae to the diffraction spectrum. It was found that the two α and γ polymorphous structures can give rise to lamellar stacks characterized by a different periodicity. In particular, the α phase has a higher value of the long period in comparison to the γ form. From the analysis of the results related to the M1, G1, and G2 samples, it was also observed that the α phase has a narrower distribution of lamellar thickness with respect to that of the γ phase.

The authors gratefully acknowledge Dr. Giampiero Morini and Dr. Luigi Resconi for providing the polypropylene samples and Dr. Fabrizio Piemontesi for precious discussions.

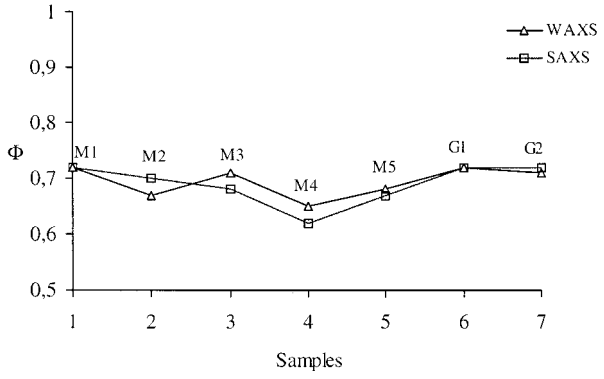

Figure 6 Comparison of WAXS and SAXS volume crystallinities.

REFERENCES

1. Natta, G.; Corradini, P.; Danusso, F.; Mantica, E.; Mazzanti, G.; Pino, P.; Moraglio, G. J Am Chem Soc 1955, 77, 1708.
2. Turner Jones, A.; Aizlewood, J. M.; Beckett, D. R. Makromol Chem 1964, 75, 134.
3. Kardos, J. L.; Christiansen, A. W.; Baer, E. J Polym Sci Part A-2 1966, 4, 777.
4. Pae, K. D.; Morrow, D. R.; Sauer, J. A. Nature 1966, 211, 514.
5. Morrow, D. R.; Newman, B. A. J Appl Phys 1968, 39, 4944.
6. Kojima, M. J Polym Sci Part A-2 1968, 6, 1255.
7. Lotz, B.; Graff, S.; Wittmann, J. C. J Polym Sci Polym Phys Ed 1986, 24, 2017.

8. Turner Jones, A. Polymer 1971, 12, 487.
9. Guidetti, G. P.; Busi, P.; Giulianelli, I.; Zannetti, R. Eur Polym J 1983, 19, 757.
10. Busico, V.; Corradini, P.; De Rosa, C.; Di Benedetto, E. Eur Polym J 1985, 21, 239.
11. Avella, M.; Martuscelli, E.; Della Volpe, G.; Segre, A.; Rossi, E.; Simonazzi, T. Makromol Chem 1986, 187, 1927.
12. Marigo, A.; Marega, C.; Zannetti, R.; Paganetto, G.; Canossa, E.; Coletta, F.; Gottardi, F. Makromol Chem 1989, 190, 2805.
13. Rieger, B.; Chien, J. C. W. Polym Bull 1989, 21, 159.
14. Rieger, B.; Mu, X.; Mallin, D. T.; Rausch, M. D.; Chien, J. C. W. Macromolecules 1990, 23, 3559.
15. Fischer, D.; Mülhaupt, R. Macromol Chem Phys 1994, 195, 1433.
16. Soga, K.; Shiono, T.; Takemura, S.; Kaminsky, W. Makromol Chem Rapid Commun 1987, 8, 305.
17. Grassi, A.; Zambelli, A.; Resconi, L.; Albizzati, E.; Mazzocchi, R. Macromolecules 1988, 21, 617.
18. Cheng, H. N.; Ewen, J. A. Makromol Chem 1989, 190, 1931.
19. Tsutsui, T.; Mizuno, A.; Kashiwa, N. Makromol Chem 1989, 190, 1177.
20. Busico, V.; Cipullo, R. J Organomet Chem 1995, 497, 113.
21. Hindeleh, A. M.; Johnson, D. J. J Phys (D) 1971, 4, 259.
22. Vonk, C. G. In Small Angle X-ray Scattering; Glatter, O.; Kratky, O., Eds.; Academic: London, 1982; p 433.
23. Vonk, C. G.; Pijpers, A. P. J Polym Sci Part B Polym Phys 1985, 23, 2517.
24. Vonk, C. G. J Appl Crystallogr 1973, 6, 81.
25. Vonk, C. G. J Appl Crystallogr 1971, 4, 340.
26. Blundell, D. J. Polymer 1978, 18, 1343.
27. Marega, C.; Marigo, A.; Cingano, G.; Zannetti, R.; Paganetto, G. Polymer 1996, 37, 5549.
28. Hosemann, R.; Bagchi, S. N. Direct Analysis of Diffraction by Matter; North-Holland: Amsterdam, 1962.
29. Frisch, H. L.; Mallows, C. L.; Bovey, F. A. J Chem Phys 1966, 45, 1565.
30. Zambelli, A.; Locatelli, P.; Bajo, G.; Bovey, F. A. Macromolecules 1975, 8, 687.
31. Ewen, J. A. J Am Chem Soc 1984, 106, 6355.
32. Resconi, L.; Fait, A.; Piemontesi, F.; Colonnesi, M.; Rychlicki, H.; Ziegler, R. Macromolecules 1995, 28, 6667.